



Contents lists available at ScienceDirect

Inorganica Chimica Acta

journal homepage: www.elsevier.com/locate/ica

Polystyrene bound dioxidovanadium(V) complexes of 2-acetylpyridine derived ligands for catalytic oxidations

Mannar R. Maurya^{a,*}, Nikita Chaudhary^a, Amit Kumar^b, Fernando Avecilla^c, João Costa Pessoa^{b,*}

^a Department of Chemistry, Indian Institute of Technology Roorkee, Roorkee 247 667, India

^b Centro de Química Estrutural, Instituto Superior Técnico, Universidade de Lisboa, Av. Rovisco Pais, 1049-001 Lisboa, Portugal

^c Departamento de Química Fundamental, Universidade da Coruña, Campus de A Zapateira, 15071 A Coruña, Spain

ARTICLE INFO

Article history:

Available online xxx

Keywords:

Vanadium complexes
Polymer-grafted vanadium complex
Crystal structure
Oxidative bromination of styrene
Oxidative bromination of *trans*-stilbene
Oxidation of benoin

ABSTRACT

Three neat complexes [V^VO₂(acpy-bhz)] (**1**) [V^VO₂(acpy-inh)] (**2**) and [V^VO₂(acpy-nah)] (**3**) and the corresponding polymer-supported (PS) dioxidovanadium(V) complexes having monobasic tridentate ONN donor ligands, abbreviated herein as PS-im[V^VO₂(acpy-bhz)] (**4**) PS-im[V^VO₂(acpy-inh)] (**5**) and PS-im[V^VO₂(acpy-nah)] (**6**) are isolated through covalent bonding of imidazolomethylpolystyrene, obtained by reacting chloromethylated polystyrene cross-linked with 5% divinylbenzene with imidazole, with the corresponding neat complexes **1–3**. All compounds are characterized in solid state and in solution, namely by spectroscopic techniques (IR, UV–Vis, ⁵¹V NMR, thermal and scanning electron micrograph studies). The monomeric form {[VO₂(acpy-nah)]·DMSO} (**3a**) of complex **3** is also isolated from its solution in DMSO and its molecular structure is confirmed by single crystal X-ray diffraction. Polymer-supported as well as neat complexes are used as catalyst precursors for the oxidative bromination of styrene and *trans*-stilbene using 30% aqueous H₂O₂ as an oxidant, the compounds acting as functional models of vanadium dependent haloperoxidases. 1-Phenylethane-1,2-diol, 2-bromo-1-phenylethane-1-ol (bromohydrin) and 1,2-dibromo-1-phenylethane are the reaction products of styrene after 1 h of reaction, while those of *trans*-stilbene are: 2,3-diphenyloxirane (*trans*-stilbene oxide), 2-bromo-1,2-diphenylethanol and 1,2-dibromo-1,2-diphenylethane. It is also shown that all these compounds are catalyst precursors for the catalytic oxidation of benzoin by peroxide, the products being benzil, methylbenzoate, benzoic acid and benzaldehyde-dimethylacetal. An outline of the mechanism is proposed and plausible intermediates involved in the catalytic processes are proposed/established by UV–Vis and ⁵¹V NMR studies.

© 2013 Elsevier B.V. All rights reserved.

1. Introduction

Immobilization of homogeneous catalysts through covalent bonding with chloromethylated polystyrene cross-linked with divinylbenzene is receiving an increasing interest for developing environmental friendly greener catalytic processes which are also economically viable in industrial chemistry [1–5]. The development of vanadium catalytic model systems for oxidations and oxygen transfer reactions, including the oxidative halogenation of organic substrates and oxidation of organic sulfides, potentiated renewed interest in the coordination chemistry of vanadium complexes with polydentate ligands [6–11].

Dioxidovanadium(V) complexes with benzimidazole, imidazole and hydrazide derived monobasic tridentate ONN ligands have

been looked at as functional models of vanadium haloperoxidases (VHPOs) [12–15]. Successful functional similarities have been demonstrated as some of these complexes mimic oxidative halogenations and sulfoxidations [14] along with the oxidation, by peroxide, of organic substrates [16].

Grafting such vanadium complexes onto polymer supports may provide extra stability to the complexes and may improve their catalytic activity and recyclable ability [1,17]. Such grafting onto polymers may also be important for the development of more environmentally benign synthetic routes to fine chemicals. For example, some of us found that polymer-supported vanadium complexes oxidize organosulfur compounds efficiently in model diesel fuels and are recyclable [15].

Two general methods have been adapted to graft vanadium complexes on polymer supports: (i) covalent bonding of a ligand to the polymer; donor atoms of this grafted ligand bind to the metal center, and (ii) the ligand bound to the metal ion possesses a functional group adequate to establish a covalent bond to the polymer. The later method has been extensively used in exploring the

* Corresponding authors. Tel.: +91 1332 285327; fax: +91 1332 273560 (M.R. Maurya). Tel.: +351 218419268; fax: +351 21 8419239 (J. Costa Pessoa).

E-mail addresses: rkmanfyc@iitr.ac.in (M.R. Maurya), joao.pessoa@ist.utl.pt (J. Costa Pessoa).

functional mimics and catalytic activities of polymer supported vanadium complexes [17], but only one report describes the former method for vanadium complexes [17,18]. In the present work we describe one more example of method (i); thus, in continuation of our efforts, herein we describe the synthesis of three polymer-supported dioxidovanadium(V) complexes of hydrazide derived monobasic tridentate ONN ligands via covalent bonding through imidazolomethylpolystyrene (cross-linked with 5% divinylbenzene) (Scheme 1). These complexes were applied to the oxidative bromination of styrene and *trans*-stilbene.

In addition, these catalyst precursors are shown to be active in the oxidation of benzoin, by peroxide. The oxidation of benzoin produces benzil, an alpha diketone that is an important organic intermediate; it has received an enormous attention because of its practical applications in organic and pharmaceutical industry such as for photosensitive and synthetic reagents. Benzil is extensively used as substrate in benzylic rearrangements and also acts as a starting material for the synthesis of many heterocyclic compounds [19,20] exhibiting biological activity e.g. the anticonvulsant derivative dilantin [21].

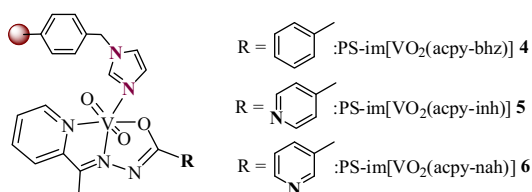
2. Experimental

2.1. Materials and methods

Chloromethylated polystyrene [18.9% Cl (5.35 mmol Cl per gram of resin)] cross-linked with 5% divinylbenzene was offered by Thermax Limited, Pune, India. Analytical reagent grade V_2O_5 , imidazole, isonicotinic acid hydrazide, hydrazine hydrate (Loba Chemie, Mumbai, India), 30% aqueous H_2O_2 , 70% $HClO_4$ (Ranbaxy, India), KBr (Himedia, India), nicotinic acid hydrazide (Fluka Chemie, Switzerland), 2-acetylpyridine and acetylacetone (Hacac) (Aldrich, USA) were used as obtained. Benzoylhydrazide was prepared by the reaction of a twofold excess of hydrazine hydrate with ethyl benzoate. Other chemicals and solvents were of analytical reagent grades. Imidazolomethylpolystyrene (PS-im) [18,22,23], $[V^{VO}(\text{acac})_2]$ [24], $[V^{VO}_2(\text{acpy-bhz})]$ (1), $[V^{VO}_2(\text{acpy-inh})]$ (2) [13] and $[\{V^{VO}(\text{acpy-nah})\}_2(\mu-O)_2]$ (3) [16] were prepared according to the reported methods. Hereafter we will abbreviate dioxidovanadium(V) as (V^{VO}_2).

2.2. Instrumentation and characterization procedures

Thermogravimetric analyses of the complexes were carried out using Perkin Elmer (Pyris Diamond) under oxygen atmosphere. Elemental analyses of the complexes were obtained with an Elementar model Vario-EL-III. Vanadium content in polymer-bound complexes was checked by Inductively Coupled Plasma spectrometry (ICP; Labtam 8440 plasma lab), as well as by TGA (see below). IR spectra were recorded as KBr pellets on a Nicolet NEXUS Aligent 1100 FT-IR spectrometer. Electronic spectra of the polymer-bound complexes were recorded in Nujol on a Shimadzu 1601 UV-Vis spectrophotometer by layering a mull of the sample on the inside of one of the cuvettes while keeping the other one layered with



Scheme 1. Schematic structure of the polymer-supported complexes used in this work.

Nujol as reference. Spectra of non-polymer bound ligands and complexes were recorded in methanol. 1H NMR spectra (on Bruker Avance III 500 MHz) and ^{51}V NMR spectra (on Bruker Avance III 400 MHz spectrometer) with the common parameter settings were recorded with samples dissolved in $DMSO-d_6$, and the δ (^{51}V) values are referenced relative to neat $V^{VO}Cl_3$ as external standard. The energy dispersive X-ray analyses (EDX) of anchored complexes were recorded on a FEI Quanta 200 FEG. The samples were coated with a thin film of gold to prevent surface charging, to protect the surface material from thermal damage by the electron beam and to make the sample conductive. A Shimadzu 2010 plus gas-chromatograph fitted with a Rtx-1 capillary column (30 m \times 0.25 mm \times 0.25 μm) and a FID detector was used to analyze the reaction products and their quantifications were made on the basis of the relative peak area of the respective product. The identity of the products was confirmed using a GC-MS Perkin-Elmer, model Clarus 500 and comparing the fragments of each product with the library available.

2.3. X-ray crystal structure determination

Single crystals of the monomeric form of **3** {now $[V^{VO}_2(\text{acpy-nah})]\cdot DMSO$ (**3a**-DMSO)} were grown in DMSO by cooling the solution at ca. 15 °C. Three-dimensional X-ray data for **3a**-DMSO were collected on a Bruker SMART Apex CCD diffractometer at 100(2) K, using a graphite monochromator and Mo $K\alpha$ radiation ($\lambda = 0.71073$ Å) by the ϕ - ω scan method. Reflections were measured from a hemisphere of data collected of frames each covering 0.3 degrees in ω . Of the 18 198 reflections measured, all of which were corrected for Lorentz and polarization effects, and for absorption by semi-empirical methods based on symmetry-equivalent and repeated reflections, 2245 independent reflections exceeded the significance level $|F|/\sigma(|F|) > 4.0$. Complex scattering factors were taken from the program package SHELXTL [25]. Crystal and structure refinement data are given in Table 1. The structures were solved by direct methods and refined by full-matrix least-squares methods on F^2 . The non-hydrogen atoms were refined with anisotropic thermal parameters in all cases. All hydrogen atoms were refined to carbon atoms, which were placed in idealized positions and refined by using a riding mode, except for C(1), C(2), C(4), C(8) and C(10) which were left to refine freely. A final difference Fourier map showed no residual density outside: 0.969 and -0.410 for **3a**-DMSO e Å^{-3} .

2.4. Preparation of polymer-supported complexes

2.4.1. PS-im $[V^{VO}_2(\text{acpy-bhz})]$ (**4**)

The Polymer-anchored PS-im (2.0 g) was allowed to swell in DMF (20 mL) for 2 h. A solution of $[V^{VO}_2(\text{acpy-bhz})]$ (1) (2.0 g, 6.47 mmol) in 25 mL DMF was added to the above suspension and the reaction mixture was heated at ca. 80 °C for 20 h with very gentle mechanical stirring. After cooling to room temperature, the dark black polymer-anchored complex was separated by filtration, washed with hot DMF followed by hot methanol and dried at 120 °C in an air oven. Yield 1.70 g (85%). Found: N, 9.26; V, 1.65%.

2.4.2. PS-im $[V^{VO}_2(\text{acpy-inh})]$ (**5**) and PS-im $[V^{VO}_2(\text{acpy-nah})]$ (**6**)

Complexes **5** and **6** were prepared analogously to **4**, replacing **1** by $[V^{VO}_2(\text{acpy-inh})]$ (2) and $[\{V^{VO}(\text{acpy-nah})\}_2(\mu-O)_2]$ (3), respectively.

Data for PS-im $[V^{VO}_2(\text{acpy-inh})]$ (**5**): Yield 1.66 g (83%). Found: N, 8.13; V, 1.36%.

Data for PS-im $[V^{VO}_2(\text{acpy-nah})]$ (**6**): Yield 1.82 g (91%). Found: N, 10.91; V, 2.06%.

Table 1
Crystal data and structure refinement for **3a**-DMSO.

	3a -DMSO
Formula	C ₁₅ H ₁₇ N ₄ O ₄ SV
Formula weight	400.33
T (K)	100(2)
λ (Å)	0.71073
Crystal system	monoclinic
Space group	P2 ₁ /n
a (Å)	9.5772(8)
b (Å)	14.3085(13)
c (Å)	12.2414(10)
β (°)	90.607(5)
V (Å ³)	1677.4(2)
Z	4
D _{calc} (g cm ⁻³)	1.585
Absorption coefficient (mm ⁻¹)	0.745
F(000)	824
Crystal size (mm ⁻³)	0.22 × 0.20 × 0.19
θ range for data collection (θ _{Min} /θ _{Max}) (°)	2.19–24.71
Index ranges	–11 ≤ h ≤ 11, –16 ≤ k ≤ 15, –14 ≤ l ≤ 13
Reflections collected	18 198
Independent reflections	2859
R _{int}	0.0698
Completeness/(θ)	99.8/(24.71°)
Refinement method	full-matrix least-squares on F ²
Restraints/parameters	2859/0/256
Goodness-of-fit (GOF) on F ²	1.047
R ₁ ^a	0.0407
wR ₂ (all data) ^b	0.1323
Largest differences peak and hole (e Å ⁻³)	0.969 and –0.410

$$^a R_1 = \frac{\sum ||F_o| - |F_c||}{\sum |F_o|}$$

$$^b wR_2 = \left\{ \frac{\sum [w(|F_o|^2 - |F_c|^2)]^2}{\sum [w(F_o^4)]} \right\}^{1/2}$$

2.5. Catalytic studies

The polymer-anchored complexes PS-im[V^VO₂(acpy-bhz)] (**4**), PS-im[V^VO₂(acpy-inh)] (**5**), PS-im[V^VO₂(acpy-nah)] (**6**) were used as catalyst precursors to carry out the oxidative bromination of styrene and *trans*-stilbene, as well as of oxidation of benzoin. Each catalyst was allowed to swell in suitable solvent (mentioned below) prior to its use.

2.5.1. Oxidative bromination of styrene

Warning! HClO₄ is potential oxidant, hence it must be handled carefully: Complexes **4–6** were used as catalyst precursors to carry out the oxidative bromination of styrene. In a typical reaction, styrene (1.04 g, 10 mmol) was added to an aqueous solution (20 mL) of KBr (3.57 g, 30 mmol) in a 100 mL reaction flask, and then 20 mL CH₂Cl₂ and 30% aqueous H₂O₂ (3.40 g, 30 mmol) were added. After adding 70% HClO₄ (1.43 g, 10 mmol) and catalyst precursors (0.0010 g), the reaction mixture was stirred at room temperature. Three additional 10 mmol portions of 70% HClO₄ were further added after every 15 min with continuous stirring. The experimental conditions (e.g. stirring speed, size of magnetic bar and reaction flask) in all batches were kept as similar as possible. After 1 h the orange colored organic layer was separated using a separatory funnel, washed with water and dried. The crude mass was re-dissolved in CH₂Cl₂ and insoluble material, if any, was removed by filtration. The solvent was evaporated and the reaction products were separated using a silica gel column. Elution of the column with 1% CH₂Cl₂ in *n*-hexane first separated a mixture of bromo derivatives, followed by 1-phenylethane-1,2-diol. The two bromo derivatives were finally separated from each other using another silica gel column and eluted with pure *n*-hexane. The products were identified by GC–MS and ¹H NMR spectra.

¹H NMR spectral data of reaction products are as follows:

1,2-Dibromo-1-phenylethane: ¹H NMR (CDCl₃): δ = 7.29–7.39 (m, 5 H, aromatic), 5.11–5.13 (q, 1 H, CH), 3.97–4.06 (septet, 2 H, CH₂) ppm.

1-Phenylethane-1,2-diol: ¹H NMR (CDCl₃): δ = 7.29–7.39 (m, 5 H, aromatic), 4.9 (q, 1 H, CH), 3.5 (q, 1 H of CH₂), 3.6 (q, 1 H of CH₂), 2.7 (br, 1 H, OH) ppm.

2-Bromo-1-phenylethane-1-ol: ¹H NMR (CDCl₃): δ = 7.29–7.39 (m, 5 H, aromatic), 5.1 (q, 1 H, CH), 3.9 (septate, 2 H, CH₂) ppm.

These data match well with those reported earlier [26,27].

2.5.2. Oxidative bromination of *trans*-stilbene

Similar procedures as outlined for styrene were applied for the oxidative bromination of *trans*-stilbene: *trans*-stilbene (0.90 g, 5 mmol), catalyst precursor (0.015 g), KBr (2.38 g, 20 mmol), 30% aqueous H₂O₂ (2.27 g, 20 mmol) and 70% HClO₄ (2.86 g, 20 mmol), added in four equal portions at time intervals (t = 0, 30, 60 and 90 min. of reaction time) were taken in CHCl₃/H₂O (40 mL, v/v). After 2 h of stirring at room temperature the orange colored organic layer was separated using a separatory funnel, washed with water and dried. The crude mass was redissolved in CH₂Cl₂; insoluble *trans*-stilbene oxide was separated by filtration and then the solvent was evaporated. Other reaction products were separated using a silica gel column. Elution of the column with 1% CH₂Cl₂ in *n*-hexane first separated a mixture of mono derivative followed by the dibromo derivative. The products were identified by GC–MS and ¹H NMR spectra.

¹H NMR spectral data of reaction products are as follows:

2,3-Diphenyloxirane: ¹H NMR (CDCl₃): δ = 7.35–7.55 (m, 10 H, aromatic); 5.5 (d, 2H, CH).

2-Bromo-1,2-diphenylethane: ¹H NMR (CDCl₃): δ = 8.0 (s, 1 H, OH); 7.37–7.52 (m, 10 H, aromatic); 5.5 (d, 2H, CH).

1,2-Dibromo-1,2-diphenylethane: ¹H NMR (CDCl₃): δ = 7.1–7.4 (m, 10 H, aromatic); 6.15 (d, 2H, CH).

2.5.3. Oxidation of benzoin

Benzoin (1.06 g, 5 mmol), 30% aqueous H₂O₂ (1.71 g, 15 mmol), and catalyst precursor (0.030 g) in 10 mL methanol were stirred at reflux temperature. The progress of the reaction was monitored by withdrawing samples at different time intervals and analyzing them quantitatively by gas chromatography. The identities of the products were confirmed by GC–MS. The effect of various parameters such as temperature, amount of oxidant and catalyst were checked to optimize the conditions for the best performance of the catalyst.

The products mainly obtained are benzil, methylbenzoate, benzoic acid and benzaldehyde-dimethylacetal.

3. Results and discussion

3.1. Synthesis, reactivity and solid state characteristics

Complexes [VO₂(acpy-bhz)] (**1**) and [VO₂(acpy-inh)] (**2**) were reported to be mononuclear while {[V^VO(acpy-nah)]₂(μ-O)₂} (**3**) to be dinuclear [16].

We obtained the monomeric form of **3** {[VO₂(acpy-nah)]-DMSO (**3a**-DMSO)}, from dimethylsulfoxide, as yellow prisms suitable for single crystal X-ray diffraction analysis. Fig. 1 shows an ORTEP representation of **3a**-DMSO and Table 2 presents selected bond lengths and angles. The complex presents an intermediate structure between the idealized square-pyramidal and trigonal-bipyramidal extremes. In fact, the geometry around the vanadium atom can be described as a distorted square-pyramidal (τ = 0.357) [28], the monobasic tridentate acpy-nah⁻ ligand binding V^V through the pyridine-N, imine-N and the amide-O and two oxido-O ligands.

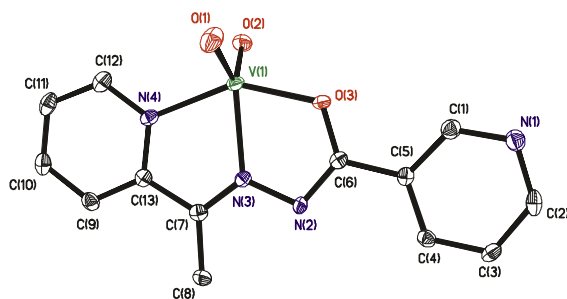


Fig. 1. ORTEP Plot of **3a**-DMSO. All the non-hydrogen atoms are presented by their 50% probability ellipsoids; hydrogen atoms are omitted for clarity.

Table 2
Bond lengths (Å) and angles (°) for [V^{VO}₂(acpy-nah)]-DMSO (**3a**-DMSO).

3a -DMSO			
<i>Bond lengths (Å)</i>			
V(1)–O(1)	1.617(2)	N(2)–N(3)	1.387(4)
V(1)–O(2)	1.619(2)	N(3)–C(7)	1.293(4)
V(1)–O(3)	1.953(2)	N(2)–C(6)	1.312(4)
V(1)–N(4)	2.097(3)		
V(1)–N(3)	2.099(3)		
<i>Bond angles (°)</i>			
O(1)–V(1)–O(2)	110.42(13)	O(1)–V(1)–N(4)	95.65(12)
O(1)–V(1)–O(3)	101.69(11)	O(2)–V(1)–N(4)	97.00(11)
O(2)–V(1)–O(3)	102.75(11)	O(3)–V(1)–N(4)	147.06(10)
O(1)–V(1)–N(3)	125.63(12)	O(3)–V(1)–N(3)	73.97(10)
O(2)–V(1)–N(3)	123.55(11)	N(4)–V(1)–N(3)	73.15(10)

The V=O distances are in the range reported for other *cis*-dioxido-vanadium(V) centers (see Table 2). The distances of the deprotonated O-atom and the N-atom of the hydrazone group to the metal ion are consistent with the values reported for other similar complexes [13,15]. It was reported that this type of VO₂-complexes can be stabilized either in the form of monomeric or dinuclear species [29]. Monomeric species can be converted to dinuclear ones upon heating in an appropriate solvent for a relatively long time. In this work the monomeric form of **3** is the relevant one.

The two external pyridine (py) rings are at an angle of 6.40(18)° with respect to each other, which is a signal of the planarity of the ligand. π - π Stacking interactions are established between the external py groups [C(1), C(2), C(3), C(4), C(5) and N(1) to C(9), C(10), C(11), C(12), C(13) and N(4)] of the acpy-nah ligand of an inversion-related molecule in the crystal packing (mean separation between the py rings ca 3.617 Å). The non coordinated py groups are also involved in π - π stacking between them, with a mean separation ca 3.783 Å, see Fig. 2.

The reaction of imidazole with chloromethylated polystyrene, cross-linked with 5% divinylbenzene in acetonitrile in the presence of KI and triethylamine, gave the imidazolomethylpolystyrene, PS-im [18,22,23]. The remaining chlorine content of 1.5% (0.42 mmol Cl per gram of resin) in the PS-im suggests ~92% loading of the imidazole. The PS-im on reaction with complexes **1–3** in DMF resulted in the formation of imidazolomethylpolystyrene-grafted V^{VO}₂-complexes: PS-im[V^{VO}₂(acpy-bhz)] (**4**), PS-im[V^{VO}₂(acpy-inh)] (**5**) and PS-im[V^{VO}₂(acpy-nah)] (**6**). The free chloromethyl groups of PS do not coordinate with the vanadium precursor. Scheme 2 presents the global synthetic procedure and Table 3 presents the vanadium loading in supported complexes.

3.2. Field emission-scanning electron microscope (FE-SEM) and energy dispersive X-ray analysis (EDX) studies

Field emission-scanning electron micrographs (FE-SEM) for single beads of pure chloromethylated polystyrene and polymer-

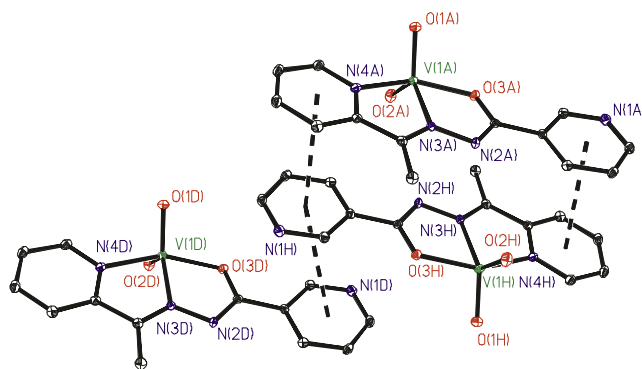


Fig. 2. Part of the crystal packing of the **3a**-DMSO. π - π Stacking interactions between pyridine groups are observed in the structure. Symmetry operations are: x, y, z ; $1/2 - x, 1/2 + y, 1/2 - z$; $-x, -y, -z$; $1/2 + x, 1/2 - y, 1/2 + z$.

grafted complex were recorded to observe the morphological changes, if any. Images of polymer-anchored complexes are reproduced in Fig. 3. Though the surface of the beads is partially damaged due to interaction of beads during anchoring, the grafting of vanadium complexes only resulted in the roughening of the top layer of polymer-anchored beads. It is not possible to obtain accurate information on the morphological changes in terms of the exact orientation of the covalently bonded metal complexes due to their poor loading. However, the estimated vanadium content of ca. 0.38 mmol g⁻¹ of resin in PS-im[V^{VO}₂(acpy-bhz)], 0.25 mmol g⁻¹ in PS-im[V^{VO}₂(acpy-inh)] and 0.39 mmol g⁻¹ of PS-im[V^{VO}₂(acpy-nah)] obtained by EDX (see Fig. S1 of Supporting information), which are close to the contents obtained through ICP-MS and TGA, suggest that the catalyst sites are uniformly distributed over the polymer upon immobilization.

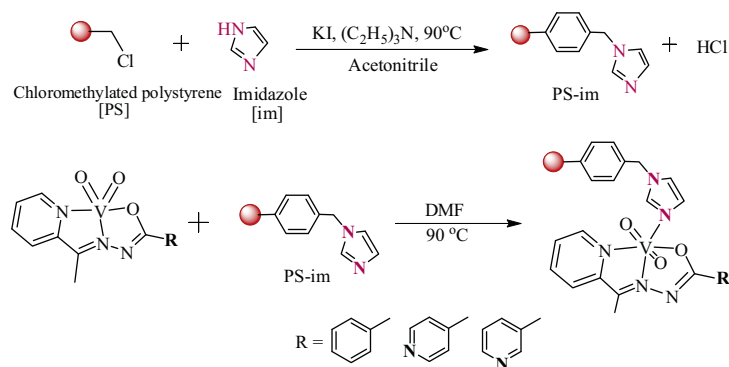
3.3. TGA studies

The polymer-bound complexes PS-im[V^{VO}₂(acpy-bhz)] (**4**), PS-im[V^{VO}₂(acpy-inh)] (**5**) and PS-im[V^{VO}₂(acpy-nah)] (**6**) are thermally stable up to ca. 200 °C. Thereafter, their thermal decomposition occurs in two exothermic but overlapping steps and is completed at ca. 550 °C. Only very small loss in weight occurs between 550–900 °C, with the formation of V₂O₅. The vanadium content calculated from the final residues are indicated in Table 3, being in agreement with those obtained by ICP-MS. As reported earlier, neat complexes **1** and **2** depict continuous degradation to V₂O₅ in the 250–700 °C temperature range [13].

3.4. IR spectral studies

The important IR bands for the neat and polymer-bound ligands and their vanadium complexes are given in Table 4. The 1500–1650 cm⁻¹ range appears quite complex in the IR of all compounds and assignments were made by comparison with previously reported results obtained from the DFT calculations recently carried out with similar types of ligands and binding sets around the vanadium center [27] (see Table 4). The ν (C=N) (azomethine) for the complexes are indicated in Table 4, the vibrations being also coupled to the aromatic ring, as was the case of [V^{IV}O(sal-ama)] complexes (sal-ama = *N*-salicylideneamino acidato) [30].

The V^{VO}₂-complexes exhibit bands due to $\nu_{\text{sym}}(\text{O}=\text{V}=\text{O})$ and $\nu_{\text{asym}}(\text{O}=\text{V}=\text{O})$ as assigned in Table 4; however, we note that recent DFT calculations for complex K[V^{VO}₂(Hdfmp(nah)₂)] {Hdfmp(nah)₂ = Schiff base obtained by the condensation of 2,6-diformyl-4-methylphenol and nicotinoylhydrazide} showed that



Scheme 2. Global synthetic procedure for the preparation of polymer bound vanadium complexes.

Table 3

Data of metal and loading in polymer-anchored complexes.

Complexes	Metal ion loading ^a (mmol g ⁻¹ of resin) (obtained by ICP)	Metal ion loading ^a (mmol g ⁻¹ of resin) (obtained by TGA)
PS-im[VO ₂ (acpy-bhz)] (4)	0.324	0.30
PS-im[VO ₂ (acpy-inh)] (5)	0.265	0.24
PS-im[VO ₂ (acpy-nah)] (6)	0.403	0.38

^a Metal ion loading = $\frac{\text{Observed metal}\% \times 10}{\text{Atomic mass of metal}}$

these two vibrations are isolated (each band corresponds to stretching of one V=O bond) [27].

Polymer supported complexes exhibit two well separated bands in the 915–940 cm⁻¹ region characteristic of *cis*-[V^VO₂] species. These bands are similar to those reported for the mononuclear neat complexes **1** and **2**. The dinuclear form of **3** displays only one band at 958 cm⁻¹ while its mononuclear analogue **3a** exhibits two sharp bands, as observed for other neat V^VO₂-complexes [17]. In polymer-supported complexes, other characteristic bands due to coordination of ligands are similar to those reported for the corresponding non-polymer-supported complexes.

3.5. Electronic spectral studies

Electronic spectral data of neat complexes have been discussed in the literature [31,32]. The polymer anchored complexes show similar spectral patterns, Fig. 4 and Table 5. The electronic spectral studies of polymer anchored complexes have been described earlier [1–5]. A band appearing at 394 nm in PS-im[V^VO₂(acpy-bhz)] is assigned to a ligand-to-metal charge transfer (lmct) transition, but may also contain bands localized in the C=N group. Thus, a medium intensity band at ca. 400 nm is assigned to *n*- π (imine) and to lmct bands. Other bands appearing in the UV region correspond to intra-ligand bands.

3.6. ⁵¹V NMR studies

Further characterization of the V^V-complexes was obtained from ⁵¹V NMR spectra recorded in DMSO-d₆. The δ_V (⁵¹V) values measured may be used to establish their behavior upon modifications of the composition of the solutions. In the present study we reinvestigated complexes **1–3a** in solution, trying to establish speciation in conditions simulating those existing during the catalytic experiments (see Scheme 3 and Table 6). All three complexes show strong resonances at ca. $\delta_V = -500$ to -505 ppm. Compound, [V^VO₂(acpy-nah)] (**3a**) was chosen as representative for the studies. The ⁵¹V NMR spectrum of **3a** (ca. 4 mM) dissolved in DMSO-d₆

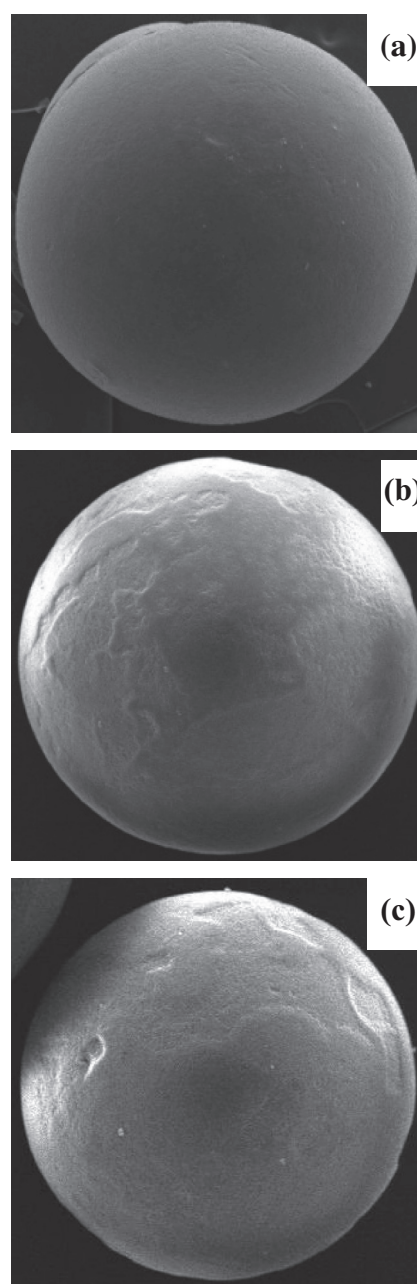


Fig. 3. FE-SEM profiles of (a) PS-im[V^VO₂(acpy-bhz)] (**4**), (b) PS-im[V^VO₂(acpy-inh)] (**5**) and (c) PS-im[V^VO₂(acpy-nah)] (**6**).

Table 4
IR spectra of compounds (ν in cm^{-1}). The DFT calculated vibrational frequencies for $\text{K}[\text{V}^{\text{V}}\text{O}_2\{\text{Hdfmp}(\text{nah})_2\}]$, scaled by a factor of 0.9, are given in parentheses [27].

Complexes	$\nu(\text{C}=\text{C}_{\text{ring}})$	$\nu(\text{C}=\text{N}_{\text{azomethine}})$	$\nu(\text{V}=\text{O})/[\text{V}-(\mu\text{-O})-\text{V}]$
$[\text{V}^{\text{V}}\text{O}_2(\text{acpy-bhz})]$ (1)	1598	1565	946, 909
$[\text{V}^{\text{V}}\text{O}_2(\text{acpy-inh})]$ (2)	1598	1565	946, 899
$[\{\text{V}^{\text{V}}\text{O}(\text{acpy-nah})\}_2(\mu\text{-O})_2]$ (3)	1600	1582	958, 778
$[\text{VO}_2(\text{acpy-nah})]\cdot\text{DMSO}$ (3a)	1595	1572	945, 898
PS-im $[\text{V}^{\text{V}}\text{O}_2(\text{acpy-bhz})]$ (4)	1600	1559	915, 926
PS-im $[\text{V}^{\text{V}}\text{O}_2(\text{acpy-inh})]$ (5)	1597	1570	920, 939
PS-im $[\text{V}^{\text{V}}\text{O}_2(\text{acpy-nah})]$ (6)	1605	1572	919, 926
$\text{K}[\text{V}^{\text{V}}\text{O}_2\{\text{Hdfmp}(\text{nah})_2\}]$		1556 (1529, 1523) [27]	934, 900 [27]

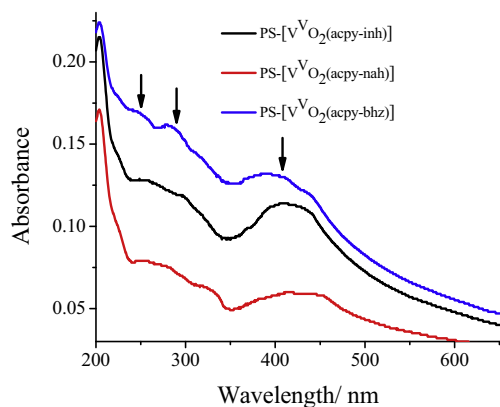


Fig. 4. Electronic spectra recorded for the polymer-anchored complexes dispersed in Nujol.

shows a strong resonance $\delta_{\text{V}} = -505$ ppm. The assignment of this and other resonances was done by considering both the experiments and comparison with DFT calculations described in previously reported studies [3,6,26,27]. Thus, the resonances at $\delta_{\text{V}} = -505$ ppm may be tentatively assigned to species such as **CI** in Scheme 3; in fact, the observed chemical shifts are within the values expected for $\text{V}^{\text{V}}\text{O}_2$ -complexes containing O/N donor sets [33,34]. Upon addition of methanol (50% v/v) to a 4 mM solution of **3** in DMSO-d_6 a new resonance at $\delta_{\text{V}} = -538$ ppm shows up; we tentatively assign this resonance to species **CI**: $[\text{V}^{\text{V}}\text{O}_2(\text{acpy-nah})(\text{S})]$, (S = solvent) [Fig. 5(b)]. Similar species were also reported, e.g. $[\text{V}^{\text{V}}\text{O}_2(\text{sal-dmenH}^+)(\text{MeOH})]$ at $\delta_{\text{V}} = -543$ ppm [2,4].

Upon additions of 0.5 and 1.0 (total) equivalents of a HCl solution a new peak at $\delta_{\text{V}} = -456$ ppm is detected [Fig. 5(c)]. We tentatively assign this resonance to species **CI**, an oxidohydroxido- V^{V} complex. Another possible assignment is **CI**, as both species correspond to the same degree of protonation, and both types of complexes have been previously considered plausible [2,4,27,32] in the case of rather similar complexes. Upon further addition of 2 equiv. of 30% H_2O_2 to this solution a resonance at $\delta_{\text{V}} = -582$ ppm is detected and could correspond to the oxido-peroxido $[\text{V}^{\text{V}}\text{O}(\text{O}_2)(\text{acpy-nahH}^+)]$ species **CI** or **CI**, Scheme 3 [Fig. 5(d)]. Similar types of $\text{V}^{\text{V}}\text{O}(\text{O}_2)$ -complexes were also considered plausible in previous studies [2,4,27,32]. However, the $\delta_{\text{V}} = -582$ ppm resonance may also correspond to the tetravanadate (**V4**) [35].

Upon addition of 30% H_2O_2 (3 equiv.) to a 4 mM solution of **3a** in DMSO-d_6 a resonance at $\delta_{\text{V}} = -588$ ppm shows up [Fig. 6(d)] which we tentatively assign as $[\text{V}^{\text{V}}\text{O}(\text{O}_2)(\text{acpy-nah})]$ (**CV**, Scheme 3); in fact this matches with the chemical shift of the authentic oxido-peroxido complexes of **3** previously reported [16]. Further additions of 3.0 equiv. KBr and 2.0 equiv. 30% H_2O_2 generates resonances at $\delta = -584$ ppm and $\delta_{\text{V}} = -601$ ppm. The resonance

Table 5
Electronic spectral data of polymer-anchored complexes.

Complexes	Solvent	λ_{max} (nm)
PS-im $[\text{V}^{\text{V}}\text{O}_2(\text{acpy-bhz})]$	Nujol	394, 277, 240
PS-im $[\text{V}^{\text{V}}\text{O}_2(\text{acpy-inh})]$	Nujol	404, 295, 253
PS-im $[\text{V}^{\text{V}}\text{O}_2(\text{acpy-nah})]$	Nujol	415, 318, 260

at $\delta_{\text{V}} = -584$ ppm is tentatively assigned to a species containing coordinated OBr^- (vanadium bound hypobromite ion) reported as probably responsible for the formation of bromohydrin (see structures **CVI**, **CVIa** or **CVIb** Scheme 3) [26,36].

The other two complexes, $[\text{V}^{\text{V}}\text{O}_2(\text{acpy-bhz})]$ (1) and $[\text{V}^{\text{V}}\text{O}_2(\text{acpy-inh})]$ (2) were also studied under similar conditions and these experiments confirmed that V^{V} species are quite stable to moderate additions of acid and/or H_2O_2 solutions, and also show similar patterns for intermediate species formation as complex **3a**. The experimental ^{51}V chemical shifts and assignments are summarized in Table 6.

Suspensions of PS- $[\text{V}^{\text{V}}\text{O}_2(\text{acpy-bhz})]$ (4), PS- $[\text{V}^{\text{V}}\text{O}_2(\text{acpy-inh})]$ (5) and PS- $[\text{V}^{\text{V}}\text{O}_2(\text{acpy-nah})]$ (6) were kept under the conditions used for the brominations of styrene and *trans*-stilbene, and then the polymer-anchored complexes were separated by filtration. ^{51}V NMR spectra were recorded for the solutions left after removing the catalyst. These solutions do not show any ^{51}V NMR resonances, suggesting that there is no leaching. We repeated this experiment up to three times at room temperature detecting no leaching by this procedure. However, under refluxing conditions these catalytic precursors partially leached into solvent and the solution show ^{51}V NMR resonances corresponding to neat complexes.

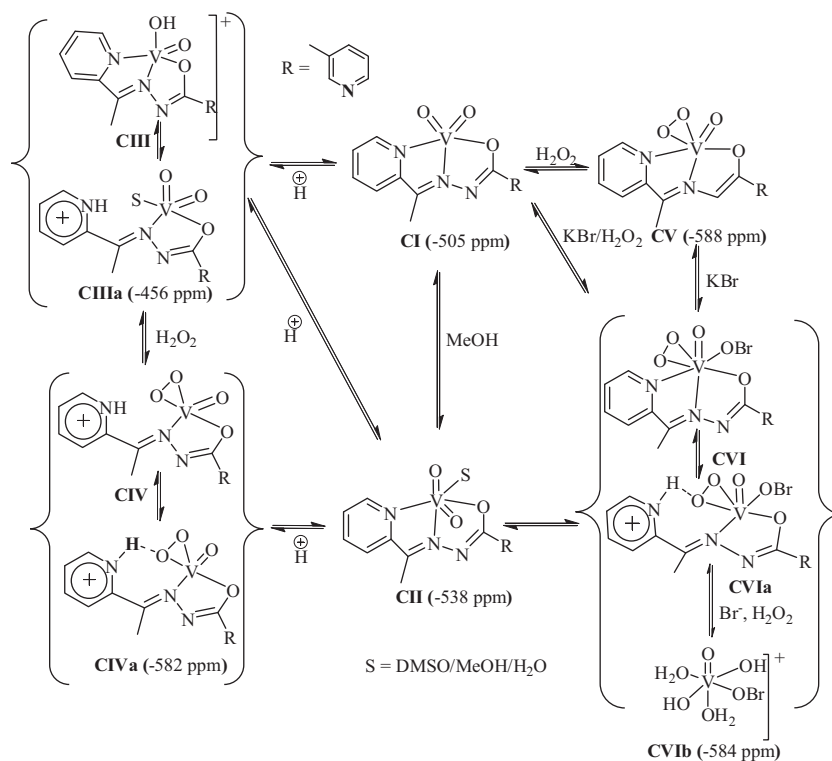
3.7. Catalytic activity studies

3.7.1. Oxidative bromination of styrene

Before use in catalytic reactions the polymer beads were swelled in CH_2Cl_2 for 4 h. For the oxidative bromination of styrene a two phase solvent system $\text{H}_2\text{O}-\text{CH}_2\text{Cl}_2$ was used, taking the polymer supported complexes as catalyst precursors in the presence of KBr, aqueous H_2O_2 and HClO_4 . Three main products were obtained: 1,2-dibromo-1-phenylethane, 2-bromo-1-phenylethane-1-ol and 1-phenylethane-1,2-diol; Scheme 4.

The obtained major products are the same as those reported by Conte et al. [36] and others [4,5,26]. Formation of some minor products such as benzaldehyde, styrene epoxide, benzoic acid and 4-bromostyrene was also observed; these are among the usual oxidation products of styrene, but their overall formation corresponds to ~5% of the total conversion of styrene. Addition of HClO_4 in four equal portions was required to obtain better yields in the oxidative bromination.

Amongst these catalyst precursors preliminary experiments showed the good catalytic activity of PS-im $[\text{V}^{\text{V}}\text{O}_2(\text{acpy-bhz})]$ (4).



Scheme 3. Summary of speciation of V^V-containing species in solutions of complex **3a**. The δ values of [V^VO₂(acpy-nah)] in DMSO-d₆ were (tentatively) established through the present ⁵¹V NMR experiments and by comparison with previous experimental and theoretical studies [2,4,26,27].

Table 6

Summary of the experimental ⁵¹V NMR data (ppm) and tentative assignments of the vanadium complexes studied in this work (see text and Scheme 3).

Complexes	CI	CII	CIII	CIV	CV	CVI
1	-504	-532	-451	-583	-591	-584
2	-500	-538	-456	-578	-591	-586
3a	-505	-538	-456	-582	-588	-584

Therefore it was taken as a representative catalyst precursor and parameters such as the amounts of catalyst, oxidant, KBr and HClO₄ were studied to optimize the reaction conditions for: (i) the maximum conversion of styrene irrespective of the selectivity of products and (ii) the maximum oxidative bromination of styrene. Taking the mixture of styrene (1.04 g, 10 mmol), KBr (3.57 g, 30 mmol) and 70% HClO₄ (5.72 g, 40 mmol) in 40 mL dichloromethane–water (1:1 v/v), five different amounts of catalyst viz. 0.010, 0.015, 0.020, 0.025 and 0.030 g were taken and the reaction was carried out at room temperature. Three additional 10 mmol portions of 70% HClO₄ were further added to the reaction mixture after every 15 min. intervals. This was necessary to avoid leaching of complex from the polymer support. As shown in Fig. 7, 0.010 g of catalyst gave 84% conversion with 6% of monobromo, 2% dibromo and 82% diol derivatives. Increasing the amount to 0.015 improved this conversion to 99% with 2% of monobromo, 6% dibromo and 84% diol derivatives. Further increasing of the catalyst did not improve the final overall conversion of the substrate; however, some impact on the selectivity of the different products was observed (entries No. 1–5 of Table 7). Therefore, an amount of 0.015 g of catalyst was selected to optimize other conditions.

The effect of amount of oxidant (30% aqueous H₂O₂) on the oxidative bromination of styrene is illustrated in Fig. 8. Under the reaction conditions of styrene (1.04 g, 10 mmol), CH₂Cl₂–H₂O (40 mL, 50% v/v), KBr (3.57 g, 30 mmol) and HClO₄ (5.72 g, 40 mmol,

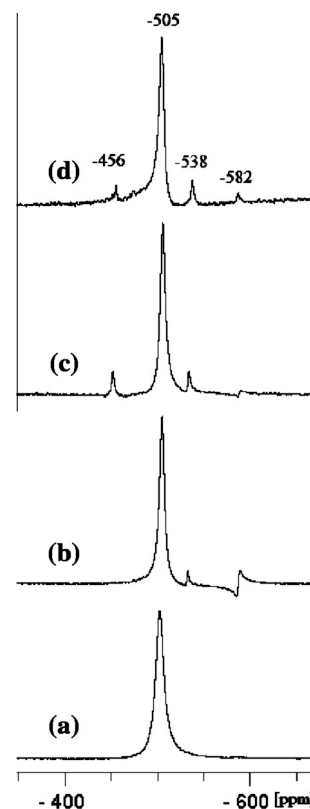


Fig. 5. ⁵¹V NMR spectra of solutions of compound **3a** (ca. 4 mM) in DMSO-d₆. (a) solution of **3a** (b) solution of (a) after addition of methanol (50% v/v); (c) solution of (b) after addition of 1.0 equiv. of HCl solution; (d) solution of (c) upon adding 2.0 equiv. of H₂O₂ (solution of 30% H₂O₂).

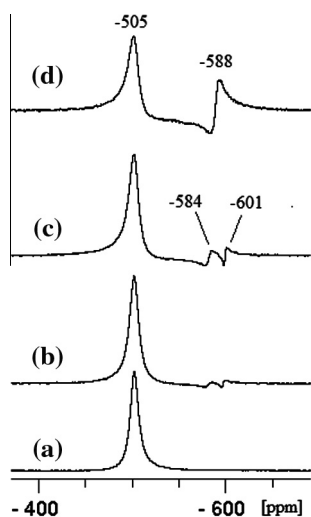
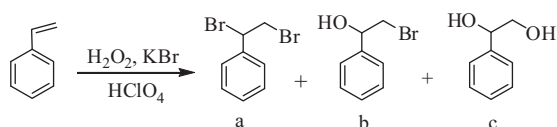


Fig. 6. ^{51}V NMR spectra of solutions of compound **3a** (ca. 4 mM) in DMSO-d_6 (a) solution of **3a**; (b) solution of (a) after addition of 3.0 equiv. KBr and 2.0 equiv. H_2O_2 (solution of 30% H_2O_2); (c) solution of (b) after ca. 15 min; (d) solution of (a) after addition of 3.0 equiv. of H_2O_2 (solution of 30% H_2O_2).



Scheme 4. Main products of catalytic oxidative bromination of styrene: (a) 1,2-dibromo-1-phenylethane, (b) 2-bromo-1-phenylethane-1-ol and (c) 1-phenylethane-1,2-diol.

added as mentioned above), a substrate to oxidant ratio of 1:1 gave 79% conversion with 48% selectivity of mono-bromo, 0% of dibromo and 51% of diol derivatives. Increasing this ratio to 1:2 improved the conversion to 99% but no improvement in the conversion was noted on further increasing this ratio (entries No. 1, 6–9 of Table 7). Therefore, a substrate to H_2O_2 ratio of 1:2 was considered suitable to optimize other conditions.

Similarly, five different amounts (viz. 20, 25, 30, 35 and 40 mmol) of KBr were used while other reaction parameters such as catalyst (0.015 g), styrene (1.04 g, 10 mmol), 30% H_2O_2 (2.27 g, 20 mmol) and HClO_4 (5.72 g, 40 mmol, added in four equal por-

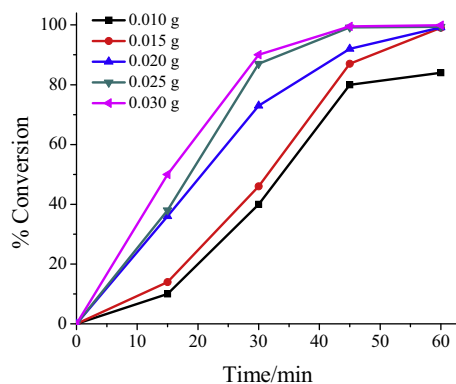


Fig. 7. Effect of the amount of catalyst $\text{PS-im}[\text{VO}_2(\text{acpy-bhz})]$ on oxidative bromination of styrene. Reaction conditions: Styrene (1.04 g, 10 mmol), $\text{CH}_2\text{Cl}_2\text{-H}_2\text{O}$ (40 mL, 50% v/v), 30% aqueous H_2O_2 (3.39 g, 30 mmol), KBr (3.57 g, 30 mmol), HClO_4 (5.72 g, 40 mmol, added in four equal portions at $t = 0, 15, 30$ and 45 min. of reaction time) at room temperature for 1 h.

tions at $t = 0, 15, 30$ and 45 min. of reaction time) in 40 mL dichloromethane-water (1:1 v/v) mixture and the reaction was monitored at room temperature for 1 h. As shown in Fig. 9, increasing the KBr amount from 20 to 25 mmol increased the conversion from 74% to 89% while 30 mmol KBr gave 99% conversion. But further increment of KBr does not make much difference in the conversion or the selectivity of the products (Entries No. 8 and 10–13 of Table 7). A 35% selectivity of mono-bromo derivative and 63% selectivity of diol derivative was obtained with 20 mmol of KBr, while 30 mmol KBr gave three main products with the following order of selectivity: diol 79% > monobromo (11%) > dibromo (5%).

The effect of various amounts of HClO_4 added in the reaction mixture as a function of the conversion of substrate is shown in Fig. 10. The way of addition of acid (here HClO_4) to the reaction mixture is made may affect the stability of the catalyst, while its amount has great influence on the conversion and selectivity of products. It was found that addition of HClO_4 successively in four equal portions at $t = 0, 15, 30$ and 45 min. of reaction time decreased the decomposition of catalyst. From the plot it is clear that 40 mmol of HClO_4 are needed to achieve 99% conversion in a period of 1 h and from the analysis of the selectivity of products we conclude that upon increasing the amount of HClO_4 it is the formation of the diol derivative that mainly increases. Equally good conversion of styrene has also been observed using H_2SO_4 under similar conditions, while the use of acetic acid was not successful.

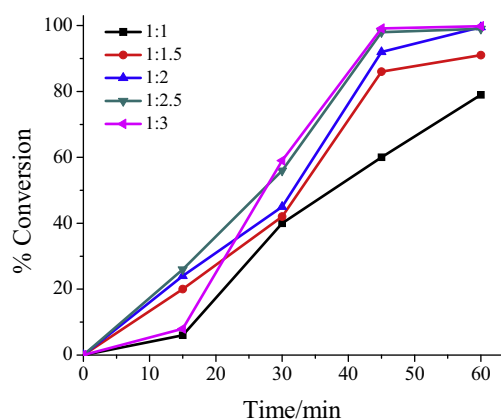
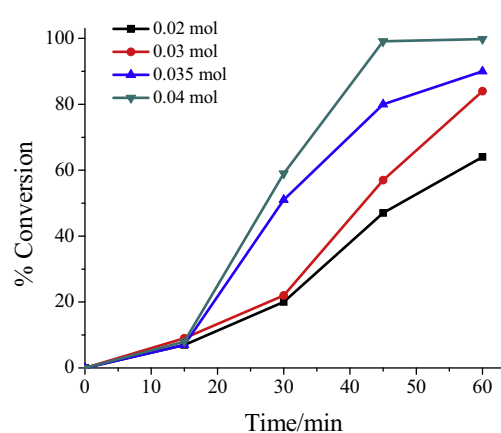
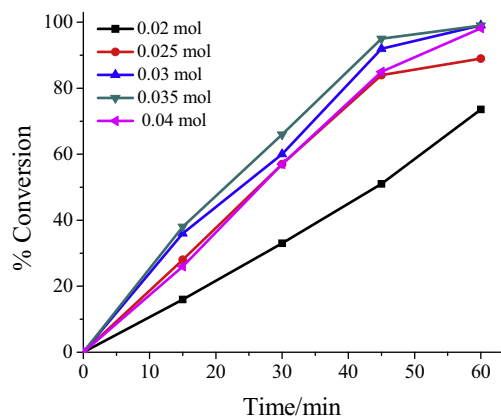
Table 7 summarizes the various reaction conditions applied to optimize the reaction conditions for the maximum oxidative bromination as well as maximum conversion of styrene considering $\text{PS-im}[\text{VO}_2(\text{acpy-bhz})]$ (**4**). Thus, the optimized reaction conditions for the maximum conversion of 10 mmol (1.04 g) of styrene are: catalyst precursor (0.015 g), 30% aqueous H_2O_2 (2.27 g, 20 mmol), KBr (3.57 g, 30 mmol), HClO_4 (5.72 g, 40 mmol, added in four equal portions at $t = 0, 15, 30$ and 45 min of reaction time) and $\text{CH}_2\text{Cl}_2\text{-H}_2\text{O}$ (40 mL, 50% v/v) at room temperature for 1 h (entry No. 8, Table 7). Entry No. 6 presents reaction conditions [i.e. styrene (1.04 g, 10 mmol) catalyst precursor (0.015 g), 30% aqueous H_2O_2 (1.135, 10 mmol), KBr (3.57 g, 30 mmol), HClO_4 (5.72 g, 40 mmol)] for the maximum formation of 2-bromo-1-phenylethane-1-ol (48% selectivity) along with 51% selectivity of diol and no formation of the dibromo derivative; however, under these conditions the maximum conversion obtained was only 79%. Reducing the amount of HClO_4 from 40 to 30 mmol (entry No. 17) improved the conversion to 96% with the formation reasonably good amount of both bromo derivatives (8% selectivity of mono bromo and 27% of dibromo) and less amount of diol (64% selectivity). Thus, lower amounts of H_2O_2 and HClO_4 both direct the reaction to the formation of bromo derivatives in satisfactory amounts.

The other two catalyst precursors, $\text{PS-im}[\text{VO}_2(\text{acpy-inh})]$ (**5**) and $\text{PS-im}[\text{VO}_2(\text{acpy-nah})]$ (**6**), along with neat complexes were also tested under the above optimized reaction conditions for the maximum conversion of styrene. The results are presented in Table 8 (and Fig. S2 of the SI section). It is clear from the data that all three supported complexes show comparable catalytic activity (94–99%); $\text{PS-im}[\text{VO}_2(\text{acpy-nah})]$ being less active. Amongst the products formed after 1 h of reaction time the selectivity of 1-phenylethane-1,2-diol is higher (76–80%) while that of 2-bromo-1-phenylethane-1-ol (bromohydrin) is 11–13%. It was observed that, extending the reaction time for another 1 h resulted in the formation of more dibromo product. These catalyst precursors were also tested for their recyclability and the results (Table 8) show that upon use they are still active and have slightly lower but equally good catalytic potential.

Details of time-on analysis i.e. the consumption of styrene and the selectivity of the formation of major products for all three catalysts are presented in Fig. 11 (and Figs. S3 and S4). Under the

Table 7Results of oxidative bromination of 1.04 g (10 mmol) of styrene after 1 h of reaction time using PS-im[V^{VO}₂(acpy-bhz)] (**4**) as catalyst precursor.

Entry No.	Catalyst (g)	KBr (g, mmol)	H ₂ O ₂ (g, mmol)	HClO ₄ (g, mmol)	Solvent (CH ₂ Cl ₂ /H ₂ O)	% Conv.	% Selectivity			
							Mono-bromo	Dibromo	Diol	Others
1	0.010	3.57, 30	3.405, 30	5.72, 40	20/20	84	6	2	82	10
2	0.015	3.57, 30	3.405, 30	5.72, 40	20/20	99	2	6	84	8
3	0.020	3.57, 30	3.405, 30	5.72, 40	20/20	99	5	4	86	5
4	0.025	3.57, 30	3.405, 30	5.72, 40	20/20	99	3	6	81	10
5	0.030	3.57, 30	3.405, 30	5.72, 40	20/20	99	3	8	80	9
6	0.015	3.57, 30	1.135, 10	5.72, 40	20/20	79	48	0	51	1
7	0.015	3.57, 30	1.69, 15	5.72, 40	20/20	91	35	2	57	6
8	0.015	3.57, 30	2.27, 20	5.72, 40	20/20	99	11	5	79	5
9	0.015	3.57, 30	2.83, 25	5.72, 40	20/20	99	12	3	80	5
10	0.015	2.38, 20	2.27, 20	5.72, 40	20/20	74	35	0	63	2
11	0.015	2.97, 25	2.27, 20	5.72, 40	20/20	89	29	2	64	5
12	0.015	4.165, 35	2.27, 20	5.72, 40	20/20	99	16	2	78	4
13	0.015	4.76, 40	2.27, 20	5.72, 40	20/20	98	12	5	79	4
14	0.015	3.57, 30	2.27, 20	2.86, 20	20/20	64	11	31	57	1
15	0.015	3.57, 30	2.27, 20	4.29, 30	20/20	84	13	22	62	3
16	0.015	3.57, 30	2.27, 20	5.00, 35	20/20	90	14	5	76	5
17	0.015	3.57, 30	1.135, 10	4.29, 30	20/20	96	8	27	64	1
18	0.015	3.57, 30	2.27, 20	2.86, 20	20/20	99	11	21	67	1

**Fig. 8.** Effect of the amount of oxidant (i.e. 30% H₂O₂) on oxidative bromination of styrene. Reaction conditions: Catalyst (0.015 g), styrene (1.04 g, 10 mmol), CH₂Cl₂/H₂O (40 mL, 50% v/v), KBr (3.57 g, 30 mmol), HClO₄ (5.72 g, 40 mmol).**Fig. 10.** Effect of the amount of HClO₄ on the oxidative bromination of styrene. Reaction conditions: Catalyst (0.015 g), styrene (1.04 g, 10 mmol), CH₂Cl₂/H₂O (40 mL, 50% v/v), H₂O₂ (2.27 g, 20 mmol), KBr (3.57 g, 30 mmol).**Fig. 9.** Effect of the amount of KBr on the oxidative bromination of styrene. Reaction conditions: Catalyst (0.015 g), styrene (1.04 g, 10 mmol), CH₂Cl₂/H₂O (40 mL, 50% v/v), H₂O₂ (2.27 g, 20 mmol), HClO₄ (5.72 g, 40 mmol).

experimental conditions presented in entry No. 8 of Table 7, the formation of 1-phenylethane-1,2-diol and 2-bromo-1-phenylethane-1-ol (bromohydrin) starts with the consumption of styrene. However, the selectivity of 1-phenylethane-1,2-diol reaches 79%

after 1 h, while that of 2-bromo-1-phenylethane-1-ol (bromohydrin) is only 12%. The formation of diol was always found to be high [26]. Either no formation of dibromo derivative or its formation in very low yield has been noted with these catalysts precursors under the above conditions. After 2 h of the reaction the selectivity of mono bromo product rolls back to nearly zero in all cases. It seems that formation of 1-phenylethane-1,2-diol occurs at the expense of the mono bromo derivative. The neat complexes are equally active and exhibit similar selectivity behavior (Table 8). However, the recycle ability of the polymer-supported complexes makes them better catalysts over non polymer-supported ones. Blank reaction gave ca. 60% oxidative bromination of styrene under above optimized reaction conditions.

Time on analysis of the results for the experimental conditions i.e. for the maximum oxidative bromination of styrene presented in entry No. 6 of Table 7 shows that the selectivity of 2-bromo-1-phenylethane-1-ol and 1-phenylethane-1,2-diol both increases with the consumption of styrene and reaches 48% and 51%, respectively, after 1 h. During the next 1 h the formation of 1,2-dibromo-1-phenylethane starts and its selectivity reaches 35%, while those of 2-bromo-1-phenylethane-1-ol and 1-phenylethane-1,2-diol reach 8% and 55%, respectively (Fig. 12).

The reaction mechanisms presented in Scheme 5 throw some light on the sequential conversion of initially formed dibromo

Table 8
Product selectivity and % conversion at optimum reaction conditions, chosen for maximum conversion of styrene.

SL.No.	Catalyst	% Conv.	Selectivity (%)				TOF (h ⁻¹)
			Mono-bromo	Dibromo	Diol	Others	
1	PS-im[V ^{VO} ₂ (acpy-bhz)] (4)	98	11	5	79	5	2016
2	PS-im[V ^{VO} ₂ (acpy-inh)] (5)	99	12	3	78	7	2037
3	PS-im[V ^{VO} ₂ (acpy-nah)] (6)	94	13	5	76	6	1934
4	PS-im[V ^{VO} ₂ (acpy-bhz)] (4) ^a	96	12	3	78	7	1954
5	PS-im[V ^{VO} ₂ (acpy-inh)] (5) ^a	97	13	4	78	5	1996
6	PS-im[V ^{VO} ₂ (acpy-nah)] (6) ^a	94	14	5	75	6	1934
7	[V ^{VO} ₂ (acpy-bhz)] (1)	97	26		73	1	1996
8	[V ^{VO} ₂ (acpy-inh)] (2)	98	30		68	2	2016
9	[V ^{VO} ₂ (acpy-nah)]-DMSO (3a)	85	36		63	1	1749
10	Blank reaction	60	15	1	80	4	–

^a Data for used catalyst (first cycle).

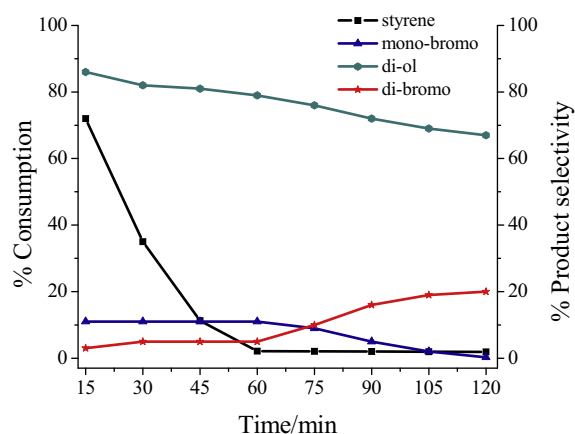


Fig. 11. Percentage consumption of styrene and selectivity of the formation of products with time using PS-im[V^{VO}₂(acpy-bhz)] (4) as catalyst precursor under the optimized conditions specified in the text. The selectivity profiles were very similar for catalyst precursors 5 and 6 (Figs. S3 and S4).

derivative into the mono-bromo one, which in turn converts into diol. Thus catalytically in situ generated HOBr, by the reaction of vanadium complex with KBr in the presence of H₂O₂ and HClO₄, reacts with styrene to give the bromonium ion as intermediate. The nucleophile Br⁻ as well as H₂O may both attack the α-carbon of the intermediate to give 1,2-dibromo-1-phenylethane and 2-bromo-1-phenylethane-1-ol, respectively. The nucleophile H₂O may further attack the α-carbon of 2-bromo-1-phenylethane-1-ol to give 1-phenylethane-1,2-diol. These steps justify the formation of 1-phenylethane-1,2-diol in highest yield under any experimental conditions mentioned in Table 7.

3.7.2. Oxidative bromination of *trans*-stilbene

Oxidative bromination of *trans*-stilbene was carried out with the biphasic chloroform–water solvent system. Chloroform was found to be better solvent in terms of solubility of *trans*-stilbene. Polymer beads were allowed to swell in chloroform for 4 h prior to the reaction. Oxidative bromination of *trans*-stilbene gave mainly three products: (i) 2,3-diphenyloxirane (TSO = *trans*-stilbene oxide), (ii) 2-bromo-1,2-diphenylethanol and (iii) 1,2-dibromo-1,2-diphenylethane; Scheme 6.

Again PS-im[V^{VO}₂(acpy-bhz)] (4) was taken as catalyst precursor and all parameters as stated above were studied in order to maximize the oxidative bromination of *trans*-stilbene. Reaction requires ca. 2 h to achieve the equilibrium. Table 9 summarizes various trials with experimental details for the oxidative bromination of *trans*-stilbene and the obtained conversions under several different reaction conditions applied.

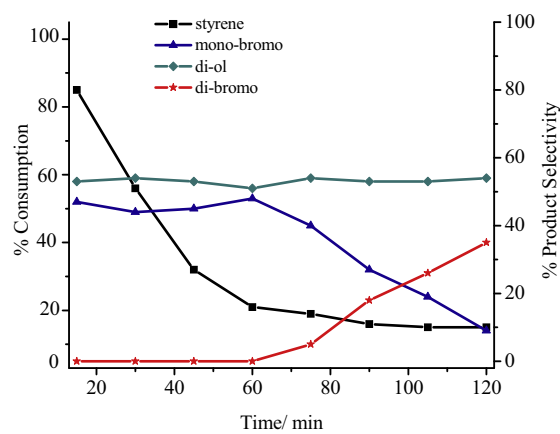
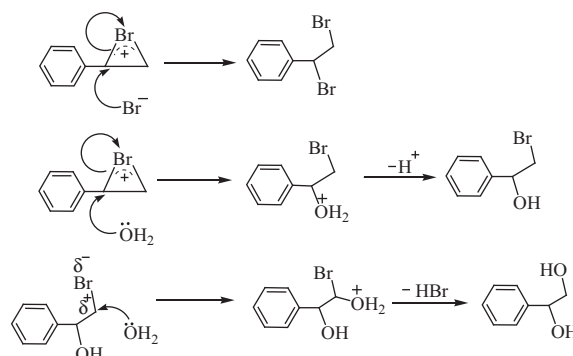
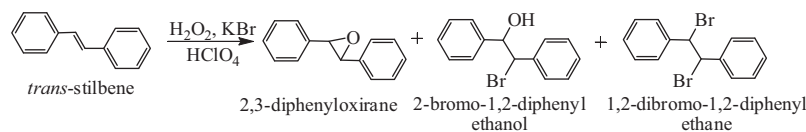


Fig. 12. Percentage consumption of styrene and selectivity of the formation of products with time using PS-im[V^{VO}₂(acpy-bhz)] (4) as catalyst precursor for the conditions of entry No. 6 in Table 7 (maximum brominated products).



Scheme 5. Possible mechanisms operating to yield the three main products detected, after the bromonium ion is formed by action of catalytically generated HOBr on styrene.

Thus, the optimized reaction conditions settled for the maximum conversion of 0.90 g (5 mmol) of *trans*-stilbene (entry No. 8; Table 9) are: catalyst precursor (0.015 g), KBr (2.38 g, 20 mmol), H₂O₂ (2.27 g, 20 mmol), HClO₄ (2.86 g, 20 mmol, added in four equal portions at *t* = 0, 30, 60 and 90 min. of reaction time) in CHCl₃–H₂O (40 mL, 1:1, v/v). Again addition of HClO₄ in four equal portions, instead of only one portion, was necessary to avoid leaching of complex from the polymer support. Under these conditions, a reasonably good amount of 2-bromo-1,2-diphenylethanol (8% selectivity) and 1,2-dibromo-1,2-diphenylethanol (26% selectivity) with a maximum of 93% conversion of *trans*-stilbene was achieved.



Scheme 6. Products of the oxidative bromination of *trans*-stilbene.

Higher amounts of oxidant does not improve the conversion of *trans*-stilbene, while higher amounts of HClO_4 causes the partial leaching of complex from the polymer support resulting in lower conversion.

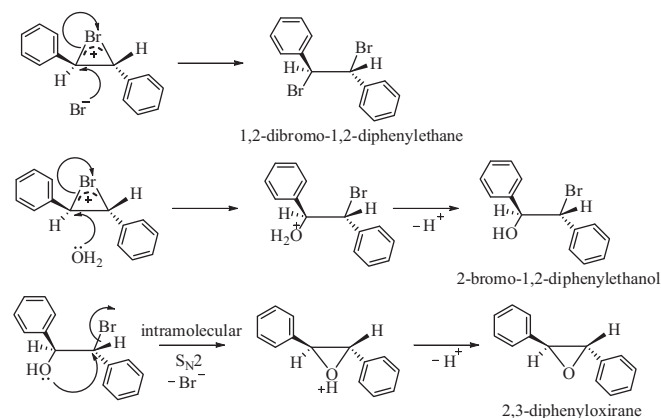
The high amount of *trans*-stilbene oxide formed under all experimental conditions presented in Table 9 led us to extend experimental trials without KBr (entry No. 10) or without catalyst (entry No. 11) under the above optimized conditions. Only 2% conversion of *trans*-stilbene was obtained in the experiments in the absence of KBr, while 55% conversion was achieved in the absence of catalyst. This suggests the importance of KBr in this reaction. Further, the formation of highest amount of *trans*-stilbene oxide (72% selectivity) in the later case led us to propose the following mechanisms (Scheme 7) for the formation of different products.

Other two polymer anchored complexes PS-im[V^{VO}₂(acpy-inh)] and PS-im[V^{VO}₂(acpy-nah)] along with non polymer-anchored complexes were also used to carry out the transformation and the results are summarized in Table 10. Under these conditions the catalytic activity of the different polymer-supported catalysts follows the order: PS-im[V^{VO}₂(acpy-inh)] (95%) > PS-im[V^{VO}₂(-acpy-bhz)] (93%) > PS-im[V^{VO}₂(acpy-nah)] (88%). In the case of the neat complexes the conversion is slightly lower [V^{VO}₂(acpy-inh)] (94%) > [V^{VO}₂(acpy-bhz)] (90%) > [V^{VO}₂(acpy-nah)] (82%) but follow the same trend and selectivity profiles. Amongst the three products formed, the selectivity of the formation of *trans*-stilbene oxide is highest (71–76%), which is followed by 1,2-dibromo-1,2-diphenylethane (22–25%) and the formation of 2-bromo-1,2-diphenylethanol is minimum.

3.7.3. Mechanism of oxidative bromination

From the mechanistic point of view involving the oxybromination reactions, one of the efforts was the elucidation of the main reaction pathway and identification of intermediates using spectroscopic techniques, namely ⁵¹V NMR.

The catalytic reactions of styrene described in this study follows the approach of using a two phase system. The mode of action of V-dependent bromoperoxidase enzymes (V-BrPOs) has received much attention [32,36–39] and it is normally accepted that vanadium, in the presence of hydrogen peroxide [40–43], forms a peroxido vanadium derivative. Oxidation of the bromide ion is followed by the formation of a bromine equivalent intermediate, which may then either brominate an organic substrate or react



Scheme 7. Proposed mechanisms operating to yield products, after the bromonium ion is formed by action of catalytically generated HOBr on *trans*-stilbene.

with another molecule of Br^- to form bromine. The primary oxidant is H_2O_2 and the role of the V^{V} ion is to serve as a strong Lewis acid in the activation process. The high efficacy of the bromination process is associated to the formation of the intermediate, and the reaction has been considered to take place in two different ‘compartments’ of the enzymes: one first step in a hydrophilic region of the protein, and the second in a hydrophobic region. This has led to model the reaction by the development of two-phase systems [31]: (1) the vanadium precursor, H_2O_2 and KBr are dissolved in water, where the formation of a V^{V} -peroxido derivative, and the oxidation of Br^- occurs with the formation of an intermediate; (2) this intermediate is transferred to the organic phase, often a chlorinated solvent (e.g. CHCl_3 or CH_2Cl_2), where the bromination of substrate takes place. The process in the aqueous phase requires acidic conditions, probably to promote the protonation of the peroxido moiety.

V^{VO} -complexes catalyze the oxidative bromination of styrene in the presence of H_2O_2 . In this reaction vanadium complexes react with 1 or 2 equiv. of H_2O_2 , forming oxidomonomerperoxido complexes which ultimately oxidize the bromide species (to Br_2 , Br_3^- and/or HOBr), the bromination of the substrate then proceeding with the liberation of a proton [37], which may act as a reservoir of the active oxidant. We clearly identified monoperoxido V^{V} -com-

Table 9

Results of oxidative bromination of 0.90 g (5 mmol) of *trans*-stilbene after 2 h of reaction time using PS-im[V^{VO}₂(acpy-bhz)] (4) as catalyst precursor.

Entry No.	KBr (g, mmol)	H_2O_2 (g, mmol)	HClO_4 (g, mmol)	Catalyst (g)	$\text{CHCl}_3/\text{H}_2\text{O}_2$ (1:1) (mL)	% Conv.	% Selectivity			
							Mono-bromo	Dibromo	TSO	Others
1	3.57, 30	3.405, 30	5.72, 40	0.015	40	91	7	15	75	3
2	3.57, 30	3.405, 30	5.72, 40	0.020	40	93	5	13	80	2
3	3.57, 30	3.405, 30	5.72, 40	0.025	40	92	6	13	79	2
4	1.18, 10	3.405, 30	5.72, 40	0.015	40	80	9	32	58	1
5	2.38, 20	3.405, 30	5.72, 40	0.015	40	95	4	22	73	1
6	2.38, 20	1.13, 10	5.72, 40	0.015	40	83	5	25	67	3
7	2.38, 20	2.27, 20	5.72, 40	0.015	40	93	4	29	65	2
8	2.38, 20	2.27, 20	2.86, 20	0.015	40	93	8	26	74	2
9	2.38, 20	2.27, 20	4.29, 30	0.015	40	95	4	26	77	3
10	0.00, 0	2.27, 20	2.86, 20	0.015	40	2	0	0	0	2
11	2.38, 20	2.27, 20	2.86, 20	–	40	55	8	15	72	5

Table 10
Results of oxidative bromination of *trans*-stilbene catalysed by different catalyst precursors. Conversion and relative amounts of products obtained after 2 h of reaction.

SL. No.	Catalyst	% Conv.	Selectivity (%)				TOF(h ⁻¹)
			Mono-bromo	Di bromo	Stilbene oxide	Others	
1	PS-im[V ^V O ₂ (acpy-bhz)] (4)	93	1	23	74	2	359
2	PS-im[V ^V O ₂ (acpy-inh)] (5)	95	1	22	74	3	366
3	PS-im[V ^V O ₂ (acpy-nah)] (6)	88	1	24	72	3	339
4	PS-im[V ^V O ₂ (acpy-bhz)] (4) ^a	91	1	20	74	5	347
5	PS-im[V ^V O ₂ (acpy-inh)] (5) ^a	94	1	23	73	3	355
6	PS-im[V ^V O ₂ (acpy-nah)] (6) ^a	86	1	25	72	2	328
7	[V ^V O ₂ (acpy-bhz)] (1)	90	1	25	71	3	347
8	[V ^V O ₂ (acpy-inh)] (2)	94	1	22	76	1	363
9	[V ^V O ₂ (acpy-nah)].DMSO (3a)	82	1	25	71	3	316

^a Data for used catalyst (first cycle).

plexes, e.g. **CV** $\delta_V = -588$ ppm Fig. 13; more details of the suggested speciation of the system are shown in Scheme 3. Upon addition Br⁻ brominated species may form (see **CVI** or **CVIa** or **CVIb**, Scheme 3) which may be responsible for the formation of bromohydrin. Accordingly, the hypobromite-like species should be directly involved in the “Br⁺” transfer process or, at least, it is one of the active species in the bromination process [38]. The occurrence, during the catalytic cycle, of a similar species, where the equatorial peroxido oxygen is protonated and the Br⁻ is prone to coordinate the other peroxido oxygen, has been proposed [39], which ultimately oxidize the bromide species (most likely to HOBr) and brominates the substrate. Therefore the halogenations may proceed involving the intermediates containing bound OBr⁻, namely the intermediates included in Scheme 3, where we tentatively suggest assignments for the resonances observed in the ⁵¹V NMR experiments to V^V-complexes containing OBr⁻ as also suggested in previous studies [27]. Hypobromite intermediates have been detected by ESI-MS on model systems [44].

It is plausible that in the present systems the V^V-catalysts act mainly to produce the bromide-containing species, e.g. a bromonium ion intermediate; the reactions then proceed to form other species, some not containing the Br atom. In the absence of a V^V-complex the reaction also proceeds with reasonable conversion, but with distinct selectivity profiles. The presence of KBr is essential to get reasonable conversion, although in many cases the brominated compounds are not the main products obtained.

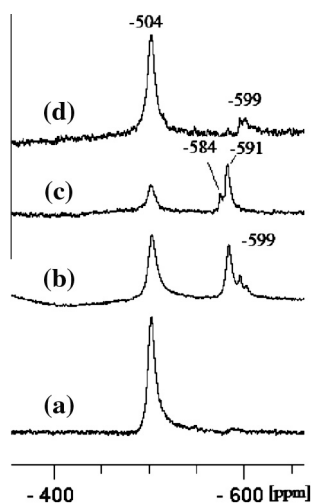


Fig. 13. ⁵¹V NMR spectra of solutions (ca. 4 mM) in DMSO-d₆ (a) of compound **1**; (b) solution of (a) after addition of 3.0 equiv. KBr and 2.0 equiv. H₂O₂ (solution of 30% H₂O₂); (c) solution of (b) after ca. 15 min. (d) solution of (a) after addition of 3.0 equiv. of H₂O₂ (solution of 30% H₂O₂).

Fig. 13 depicts ⁵¹V NMR experiments with catalytic precursors upon additions of H₂O₂ and KBr. New resonances appear at -584 ppm (and at -599 to -601 ppm). The resonance observed here at $\delta_V = -584$ ppm is tentatively assigned to a species containing coordinated OBr⁻ which, as mentioned, could be responsible for the formation of the bromohydrin (see structures **CVI**, **CVIa** or **CVIb** Scheme 3). Therefore the halogenations may indeed proceed involving the intermediates outlined in Scheme 3. However, the resonance at $\delta_V \approx -584$ ppm may also be ascribed to other formulations not containing bound hypobromite ion, thus definite assignments for these resonances cannot be made in the present systems.

3.7.4. Oxidation of benzoin

The production of benzil from benzoin has attracted much attention, as benzil is a particularly useful intermediate for the synthesis of heterocyclic compounds and benzylic acid rearrangements [4,45–47]. The catalytic oxidation of benzoin was achieved successfully with these polymer-supported complexes using 30% aqueous H₂O₂ as oxidant. The polymer beads were allowed to swell in methanol for 2 h prior to the reaction. The main products obtained were: benzil, methylbenzoate, benzoic acid and benzaldehyde-dimethylacetal; Scheme 8.

To optimize the reaction conditions for the maximum oxidation of benzoin, the effect of various amounts of catalyst on the oxidation of benzoin for the fixed conditions of: benzoin (1.06 g, 5 mmol) and 30% H₂O₂ (1.13 g, 10 mmol) in 15 mL of methanol at reflux temperature was studied as a function of time for 6 h and the results are illustrated in Fig. 14. Increasing the catalyst precursor amount from 0.010 to 0.015 g increases the conversion from 56% to 69%. This conversion further improved to 74% on increasing the catalyst amount to 0.020 g, but no significant improvement in the conversion was noted on further increasing its amount. Therefore an amount of 0.020 g was considered the best for optimum conversion of benzoin in 6 h of reaction time, and the experiments described below were carried out using this amount of catalyst precursor.

Variation in the volume of the solvent was also studied by taking 10, 15 and 20 mL of methanol; Fig. 15. It was observed that 15 mL of methanol for 1.06 g (5 mmol) of benzoin, 0.020 g of catalyst and 1.13 g 30% H₂O₂ was sufficient enough to carry out the reaction at reflux temperature for satisfactory transformation (73%) of benzoin.

The effect of amount of oxidant was studied considering three different benzoin to H₂O₂ molar ratios of 1:1, 1:2 and 1:3 under the above optimized conditions i.e. amount of benzoin (1.06 g, 5 mmol) and PS-im[V^VO₂(acpy-bhz)] (0.020 g) in refluxing methanol (15 mL). A maximum of 87.0% conversion was achieved at a benzoin to H₂O₂ molar ratio of 1:3 in 6 h of reaction time while 1:1 and 1:2 ratios resulted in 60.0% and 75.0% conversion,

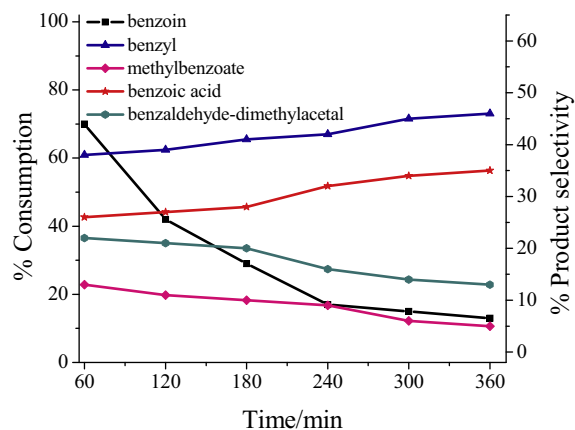


Fig. 17. Percentage conversion of benzoin and selectivity of the formation of products with time using PS-im[V^{VO}₂(acpy-bhz)] (4) as catalyst precursor under the optimized conditions specified in the text.

all four products start from the beginning of the consumption of the benzoin. The consumption of benzoin is relatively fast for the first 4 h (83%) and within the next 2 h reaches 87% (at the end of 6 h). Similarly, the rate of formation of benzil is highest among all the products up to 4 h (35%) and then improves slowly for the remaining 2 h (up to 40%). Methyl benzoate, benzoic acid and benzaldehyde-dimethylacetal form slowly for initial 1 h (3%, 2% and 1%, respectively); after that the amount of methyl benzoate increases more rapidly, with 30% formation at the end of 5 h. The amounts of benzoic acid and benzaldehyde-dimethylacetal increase very slowly throughout the 6 h of reaction, with an overall 11% and 5% formation, respectively, till the end of the process.

Similar trends were observed for PS-im[V^{VO}₂(acpy-inh)] (5) and PS-im[V^{VO}₂(acpy-nah)] (6) (Figs. S5 and S6 of SI section). For PS-im[V^{VO}₂(acpy-inh)], the percentage product formation of benzil, methylbenzoate, benzoic acid and benzaldehyde-dimethylacetal is 42%, 30%, 10%, 7%, respectively with 90% consumption of benzoin. For PS-im[V^{VO}₂(acpy-nah)] (5) the percentage product formation of benzil, methylbenzoate, benzoic acid and benzaldehyde-dimethylacetal is 40%, 24%, 11%, 5%, respectively, with 81% consumption of benzoin at the end of 6 h.

4. Conclusions

Three potentially polymer-supported (PS) V^{VO}₂-complexes with ONN donor ligands, abbreviated herein as PS-im[V^{VO}₂(acpy-bhz)] (4) PS-im[V^{VO}₂(acpy-inh)] (5) and PS-im[V^{VO}₂(acpy-nah)] (6), were designed, synthesized and characterized. The corresponding neat complexes were also characterized by analytical and spectroscopic techniques. A monomeric version of complex 3 was also characterized by single crystal X-ray diffraction analysis.

The prepared V^{VO}₂-complexes, polymer-supported as well as neat complexes, were successively used as catalyst precursors for the oxidative bromination of styrene and *trans*-stilbene using 30% aqueous H₂O₂ as an oxidant. Thus these V^V-complexes may be considered as functional models of VHPOs. Their catalytic potential for benzoin oxidation was also demonstrated. The polymer-supported catalysts are thermally more stable, selective, easy recoverable from the reaction mixture and recyclable without much decrease of activity. Interestingly, reactions take place in the absence of the vanadium complexes, with moderate conversions of the substrates, but the selectivity profiles of the reaction products differ; namely much lower amounts of brominated products are obtained. In the absence of KBr almost no conversion of

e.g. *trans*-stilbene was achieved under the experimental conditions used.

The complexes can also be converted, by treatment with H₂O₂, to the corresponding peroxido-complexes, similar to what is expected to be one of the intermediates in the catalytic cycle of the activity of VHPO. ⁵¹V NMR experiments with DMSO solutions of the neat complexes, by adding methanol, acid, KBr and/or H₂O₂ allowed to detect several distinct V^{VO}₂⁻, V^{VO}₂⁻, V^{VO}(OH)⁻ and V^V-O(O₂)-species in solution. Some of these, namely the V^{VO}(O₂)-L and species probably containing coordinated OBr⁻, are plausible intermediates in the catalytic reactions to produce the bromine-containing intermediates.

Acknowledgements

MRM thank the Department of Science and Technology, the Government of India, New Delhi for financial support of the work (SR/S1/IC-32/2010). NC acknowledge Council of Scientific and Industrial Research, New Delhi for fellowship. JCP and AK thank FEDER, Fundação para a Ciência e Tecnologia, the Portuguese NMR Network (IST-UTL Center), RECI/SEQ-QIN/0189/2012, PEst-OE/QUI/UI0100/2013 and SFRH/BPD/90976/2012.

Appendix A. Supplementary material

CCDC 956751 contains the supplementary crystallographic data for this paper. These data can be obtained free of charge from The Cambridge Crystallographic Data Centre via www.ccdc.cam.ac.uk/data_request/cif. Supplementary data associated with this article can be found, in the online version, at <http://dx.doi.org/10.1016/j.ica.2013.11.021>.

References

- M.R. Maurya, A. Kumar, J. Costa Pessoa, *Coord. Chem. Rev.* 255 (2011) 2315; M.R. Maurya, U. Kumar, I. Correia, P. Adao, J. Costa Pessoa, *Eur. J. Inorg. Chem.* (2008) 577; (c) M.R. Maurya, U. Kumar, P. Manikandan, *Eur. J. Inorg. Chem.* (2007) 2303.
- M.R. Maurya, A. Arya, A. Kumar, F. Aveilla, J. Costa Pessoa, *Inorg. Chem.* 49 (2010) 6586.
- M.R. Maurya, A. Arya, A. Kumar, J. Costa Pessoa, *Dalton Trans.* (2009) 9555.
- M.R. Maurya, A. Arya, A. Kumar, J. Costa Pessoa, *Dalton Trans.* (2009) 2185.
- M.R. Maurya, M. Kumar, A. Kumar, J. Costa Pessoa, *Dalton Trans.* (2008) 4220.
- A.G.J. Ligtenberg, R. Hage, B.L. Feringa, *Coord. Chem. Rev.* 237 (2003) 89.
- V. Conte, F. Di Furia, G. Licini, *Appl. Catal. A* 157 (1997) 335.
- A. Butler, M.J. Clague, G.E. Meister, *Chem. Rev.* 94 (1994) 625.
- M.R. Maurya, *Coord. Chem. Rev.* 237 (2003) 163.
- D. Rehder, *Bioinorganic Vanadium Chemistry*, Wiley, New York, 2008.
- G. Zampella, P. Fantucci, V.L. Pecoraro, L. De Gioia, *J. Am. Chem. Soc.* 127 (2005) 953.
- D.C. Crans, A.D. Keramidis, S.S. Amin, O.P. Anderson, S.M. Miller, *J. Chem. Soc., Dalton Trans.* (1997) 2799.
- M.R. Maurya, S. Khurana, W. Zhang, D. Rehder, *J. Chem. Soc., Dalton Trans.* (2002) 3015.
- M.R. Maurya, A. Kumar, M. Ebel, D. Rehder, *Inorg. Chem.* 45 (2006) 5924.
- M.R. Maurya, A. Arya, U. Kumar, A. Kumar, J. Costa Pessoa, *Dalton Trans.* 39 (2010) 1345.
- M.R. Maurya, S. Agarwal, M. Abid, A. Azam, C. Bader, M. Ebel, D. Rehder, *Dalton Trans.* (2006) 937.
- M.R. Maurya, J. Costa Pessoa, *J. Organomet. Chem.* 696 (2011) 244.
- M.R. Maurya, M. Kumar, A. Arya, *Catal. Commun.* 10 (2008) 187.
- H. Wynberg, H.J. Kooreman, *J. Am. Chem. Soc.* 87 (1965) 1739.
- W.W. Paudler, J.M. Barton, *J. Org. Chem.* 31 (1966) 1720.
- W.R. Dunnivant, F.L. James, *J. Am. Chem. Soc.* 78 (1956) 2740.
- G. Grivani, S. Tangestaninejad, M.H. Habibi, V. Mirkhani, M. Moghadam, *Appl. Catal. A: Gen.* 299 (2006) 131.
- S. Tangestaninejad, M.H. Habibi, V. Mirkhani, G. Grivani, *J. Mol. Catal. A: Chem.* 255 (2006) 249.
- R.A. Row, M.M. Jones, *Inorg. Synth.* 5 (1957) 113.
- G.M. Sheldrick, SHELXL-97: An Integrated System for Solving and Refining Crystal Structures from Diffraction Data (Revision 4.1), University of Göttingen, Germany, 1997.
- M.R. Maurya, C. Haldar, A.A. Khan, A. Azam, A. Salahuddin, A. Kumar, J. Costa Pessoa, *Eur. J. Inorg. Chem.* (2012) 2560.

- [27] M.R. Maurya, C. Haldar, A. Kumar, M. Kuznetsov, F. Avecilla, J. Costa Pessoa, *Dalton Trans.* 42 (2013) 11941.
- [28] A.W. Addison, T.N. Rao, J. Reedijk, J. Rijn, G.C. Verschoor, *J. Chem. Soc., Dalton Trans.* (1984) 1349.
- [29] (a) M.R. Maurya, A. Kumar, A.R. Bhat, A. Azam, C. Bader, D. Rehder, *Inorg. Chem.* 45 (2006) 1260;
(b) M.R. Maurya, A. Kumar, M. Abid, A. Azam, *Inorg. Chim. Acta* 359 (2006) 2439.
- [30] J. Costa Pessoa, M.J. Calhorda, I. Cavaco, I. Correia, M.T. Duarte, V. Felix, R.T. Henriques, M.F.M. Piedade, I. Tomaz, *J. Chem. Soc., Dalton Trans.* (2002) 4407.
- [31] M.R. Maurya, S. Khurana, W. Zhang, D. Rehder, *Eur. J. Inorg. Chem.* (2002) 1749.
- [32] M.R. Maurya, S. Agarwal, C. Bader, M. Ebel, D. Rehder, *Dalton Trans.* (2005) 537.
- [33] (a) D. Rehder, C. Weidemann, A. Duch, W. Priebsch, *Inorg. Chem.* 27 (1988) 584;
(b) O.W. Howarth, *Prog. Magn. Reson. Spectrosc.* 22 (1990) 453.
- [34] D. Rehder, in: P.S. Pregosin (Ed.), *Transition Metal Nuclear Magnetic Resonance*, Elsevier, New York, 1991, p. 1.
- [35] (a) M. Aureliano, R.M.C. Gandara, *J. Inorg. Biochem.* 99 (2005) 979;
(b) M. Aureliano, T. Tiago, R.M.C. Gandara, A. Sousa, A. Moderno, M. Kaliva, A. Salifoglou, R.O. Duarte, J.J.G. Moura, *J. Inorg. Biochem.* 99 (2005) 2355.
- [36] (a) V. Conte, B. Floris, *Inorg. Chim. Acta* 363 (2010) 1935;
(b) V. Conte, A. Coletti, B. Floris, G. Licini, C. Zonta, *Coord. Chem. Rev.* 255 (2011) 2165.
- [37] B.J. Hamstra, G.J. Colpas, V.L. Pecoraro, *Inorg. Chem.* 37 (1998) 949.
- [38] M.J. Clague, N.L. Keder, A. Butler, *Inorg. Chem.* 32 (1993) 4754.
- [39] G. Zampilla, P. Fantucci, V.L. Pecoraro, L. De Gioia, *J. Am. Chem. Soc.* 127 (2005) 953.
- [40] C.R. Cornman, J. Kampf, M.S. Lah, *Inorg. Chem.* 31 (1992) 2035.
- [41] L.J. Calviou, J.M. Arber, D. Collison, C.D. Garner, W. Clegg, *J. Chem. Soc., Chem. Commun.* (1992) 654.
- [42] A.D. Keramidias, S.M. Miller, O.P. Anderson, D.C. Crans, *J. Am. Chem. Soc.* 119 (1997) 8901.
- [43] V. Conte, O. Bortolini, M. Carraro, S. Moro, *J. Inorg. Biochem.* 80 (2000) 41.
- [44] O. Bortolini, M. Carraro, V. Conte, S. Moro, *Eur. J. Inorg. Chem.* (2003) 42.
- [45] G.B. Gill, in: G. Pattenden (Ed.), *Comprehensive Organic Synthesis*, vol. 3, Pergamon Press, New York, 1991, pp. 821–838.
- [46] M. Weiss, *J. Am. Chem. Soc.* 70 (1948) 3666.
- [47] W.-Y. Sun, *Tetrahedron* 48 (1992) 1557.